First Results of the Sideband-Separating Mixer for ALMA Band 9 Upgrade

Andrey Khudchenko, Ronald Hesper, Andrey Baryshev, F. Patricio Mena, Gerrit Gerlofma, Tony Zijlstra, Teun M. Klapwijk, Jacob W. Kooi and Marco Spaans

***Abstract*—Last year, the design and implementation details of a new modular sideband-separating mixer block, intended as an upgrade for the current single-ended ALMA Band 9 mixers, were presented at this conference. In high-frequency observation bands like ALMA Band 9 (600—720 GHz), which is strongly influenced by atmospheric noise, employment of sideband-separating mixers can reduce, by roughly a factor of two, the integration time needed to reach a certain signal-to-noise ratio for spectral line observations. Alternatively, in the same integration time, a sufficiently larger selection of sources can be accessed.**

Two prototype mixer blocks were produced on a micro milling machine, and equipped with production Band 9 SIS mixer devices that have independently been tested in double-sideband mode.

Here, we present the results of the first measurements, notably, the noise temperature, image rejection, LO pumping balance and IF response. We also present in detail a procedure of the image rejection ratio measurement, which is fast and can be used for single sideband mixers, so that a second IF chain is not required.

***Index Terms*—Image rejection ratio, sideband separating mixers, submillimeter mixers, superconductor-insulator-superconductor junction**

I. Introduction

THE possibility of reducing the atmospheric noise by a factor of two and increase as result a signal to noise ratio of about 1.4 times is the motivation for ALMA Band 9 mixers upgrade form dual sideband (DSB) to single sideband (SSB) mode.

Manuscript received August 1, 2011. This work was supported.in part: by the ESO Band9 Upgrade Study PO-037021; European Community Framework Program 7, Advanced Radio Astronomy in Europe, AMSTAR+, grant agreement no. 227290; Dutch NWO/STW VENI Grant 08119, "Advanced Heterodyne Mixers for THz Applications", Dutch research school for astronomy (NOVA) NOVAIII Grant; Center of Excellence in Astrophysics and Associated Technologies (PBF 06), Chilie.

A. Khudchenko and A. Baryshev are with Netherlands Institute for Space Research SRON, Landleven 12, 9747 AD Groningen, The Netherlands, (+31 50 363 4018, A.Khudchenko@sron.nl).

R. Hesper, A. Baryshev, G. Gerlofma and M. Spaans with Kapteyn Astronomical Institute, Landleven 12, 9747 AD Groningen, The Netherlands

P Mena with Electrical Engineering Department, Universidad de Chile, Av. Tupper 2007, Santiago, Chile

Tony Zijlstra, Teun M. Klapwijk are with Kavli Institute of Nanoscience, Delft University of Technology, Lorentzweg 1, 2628 CJ Delft The Netherlands

J.W. Kooi with California Institute of Technology, MS 320-47 Pasadena, CA 91125, USA is with the National Institute of Standards and Technology, Boulder, CO 80305 USA.

Because the ALMA correlator can only handle 8 GHz of intermediate frequency (IF) bandwidth per polarization, an SSB configuration with 4-12 GHz IF has been chosen [1], rather than a full two sideband (2SB) one, split over two 4 GHz bands. Also, in this way the existing DSB IF chain does not have to be modified for the upgrade, i.e., all the IF components can be reused. The only IF component to be added is one IF hybrid per polarization.

The mechanical design of the SSB receiver was presented in [1]. The manufactured modular block is shown in Fig. 1. There are a few key features in this design. First of all, it is as modular as reasonably possible. Especially the holders containing the junctions are easily separable from the RF hybrid block. The standard single-ended Band 9 junction holders ("back pieces") are used, so that junctions can be tested individually and easily matched. It means that no development of a new junction design is required. The SIS mixers are made in Nb/AlN/Nb technology. The mixer block is also compact: 45x21x53 mm^3 (see Fig. 1), so the upgrade mixers can be retrofitted into the existing optics blocks with minimal reworking.

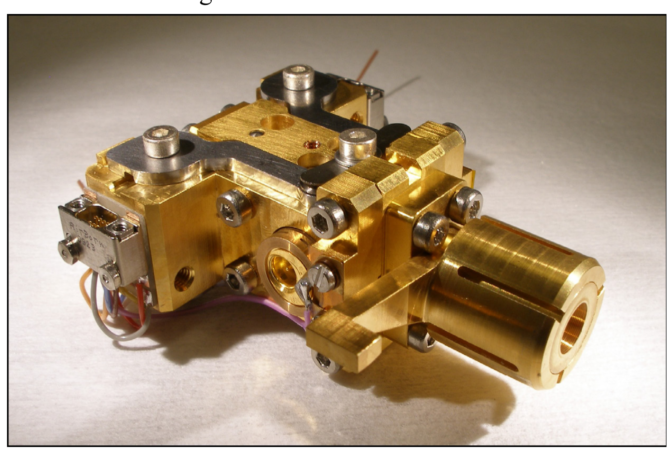

Fig. 1. Photograph of the first SSB mixer. The corrugated RF input horn is on the right, the LO horn is on the back site opposite to it (not visible). One of the standard band 9 mixer back pieces is visible near the center.

In this paper, we present the results of the first measurements performed to characterize this mixer. The properties of the RF hybrid and LO splitter were studied in a direct way, by measuring the balance of pumping levels, both through the LO port and the RF port. Moreover, the frequency response, noise temperature and sideband rejection ratio were also measured. Finally, we describe in detail a new procedure for measuring the image rejection ratio, which is fast and can be used for a SSB mixer so that a second IF chain is not required.

II. Mixer Characterization

A. RF Hybrid

Since the new design uses standard ALMA Band 9 back pieces to hold the SIS junctions, the RF response of each SIS junction can be measured before the installation into the sideband-separating mixer block. A comparison between the frequency responses of the same two SIS mixers in single-ended DSB configuration (production ALMA Band 9 mixer) and in the sideband separating mixer block is presented in Fig. 2. The responses are measured using a Fourier-transform spectrometer. Since the response is measured by way of the mixer bias current, the IF output hybrid does not come into play.

Comparing the spectra taken through the 2SB block (solid lines) with the ones taken with the individual SIS mixer devices (DSB mode, dashed lines) shows that the waveguide structure (consisting of RF hybrid and LO couplers) does not dramatically influence the RF response and covers the required band (600-720 GHz).

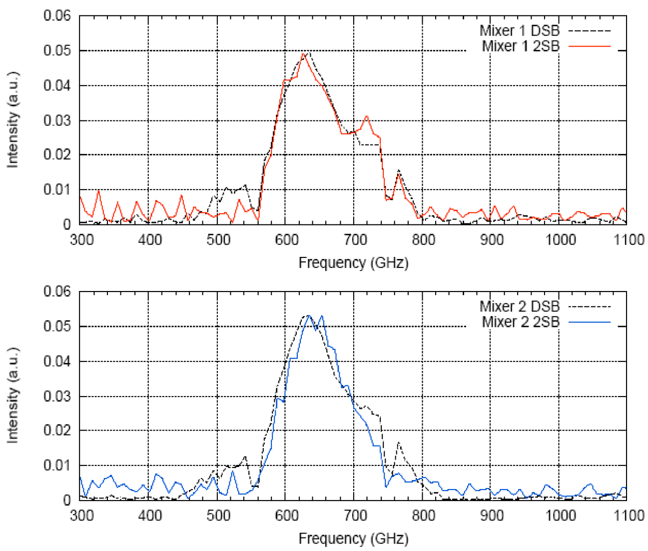

Fig. 2. Direct RF response of the SIS mixers: dashed lines – individual DSB response; solid lines - response of the junctions installed in the 2SB RF hybrid block.

Fig. 3 characterizes the transmission balance of the RF hybrid and LO splitter, measured by injecting the LO signal through, respectively, the RF and LO horns, and measuring the SIS bias current. Since the bias current of a pumped SIS junction at a fixed bias voltage in this regime is proportional to the RF power reaching the junction [2], the ratio of the currents is equal to the power ratio, independent of frequency or absolute LO power.

The curve measured with the signal injected through the LO port shows a periodic frequency-dependent imbalance in the LO distribution structure (LO splitter, couplers and dummy loads), indicating that standing waves may be present. This imbalance prevents both mixers to be pumped optimally at the same time. However, since around the optimal pumping level the noise performance of an SIS mixer is not very strongly dependent on LO power, deviations of less than about 20% (1 dB) are acceptable. Both the LO and RF coupling ratios, shown in Fig. 3, are within ±1.5 dB, which is not too far from that level. However, the real impact should be judged from noise temperature and sideband ratio measurements. Small imbalances can be compensated by adjusting the bias voltages (and thereby the mixer gains) of the individual SIS devices, though possibly with a certain degradation of the noise temperature.

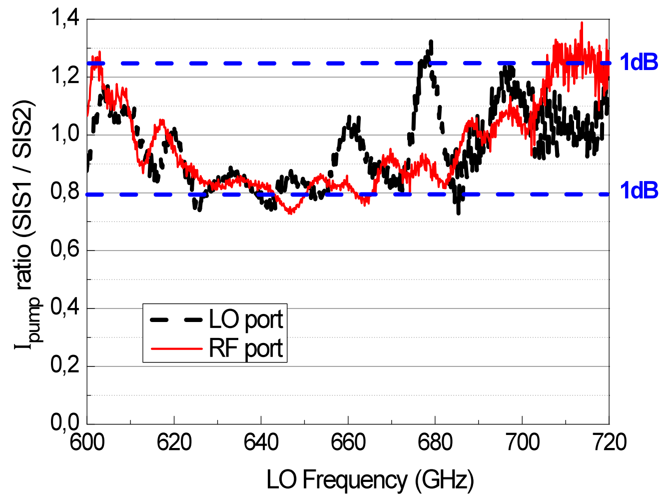

Fig. 3. Pumping balance between the two SIS devices in the mixer block, measured as the ratio of the SIS pumping currents at constant bias voltage while sweeping the LO frequency, both through the RF port and the LO port. Ideally, these ratios should be 1.

B. IF Hybrid and IF Chain

The preliminary tests of the IF chain were performed with 4-8 GHz cryogenic amplifiers as described in [3]. Here we present results for the 4-12GHz IF chains, based on the Yebes cryogenic amplifiers used in the ALMA Band 9 DSB cartridge. The 90 degree 4-12GHz IF hybrid (provided by Observatorio Astronómico Nacional, Spain [4]) is placed between the SIS junctions and the 4-12 GHz isolators before the amplifiers. The hybrid has an amplitude imbalance less than ±0.3 dB and phase imbalance not exceeding ±2 degrees, over the 4-12 GHz band.

The performance of the entire IF chain (including the IF microstrip structure on the mixer devices, IF hybrid, isolators and amplifiers) was determined, by using the SIS junctions as noise sources, biasing them at different voltages above the gap (5 and 8 mV in this case). Since the level of the shot noise generated by a SIS junction is known, we can determine the individual noise contributions by measuring the IF output spectra in three (out of four) bias combinations: 5 and 5 mV; 5 and 8 mV; 8 and 5 mV (for the first and the second SIS junctions correspondingly).

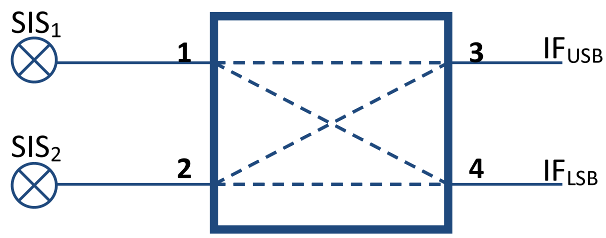

Fig. 4. Block diagram of the IF chains.

The measured IF spectra can be presented in accordance with the diagram in Fig. 4 in the following way (for either IF output):

$$P_{5-5} = (P_1 G_{31} + P_2 G_{32} + P_N) G_{IF},$$
$$P_{5-8} = (P_1 G_{31} + K P_2 G_{32} + P_N) G_{IF},$$
$$P_{8-5} = (K P_1 G_{31} + P_2 G_{32} + P_N) G_{IF},$$

where G_{ij} is the power gain between ports j and i; P_1 and P_2 are the shot noise powers of the SIS mixers at 5 mV; K is the factor of shot noise increase when the SIS junction bias is increased from 5 to 8 mV; G_{IF} is the gain of the IF chain after the hybrid; P_N is the noise power of the IF amplifiers. The presented equations are valid for both IF chains. By selecting the SIS junctions to have the same gap currents I_g, we can make $P_1=P_2$. Under this condition the following ratio can be derived:

$$\frac{G_{31}}{G_{32}} = \frac{P_{8-5} - P_{5-5}}{P_{5-8} - P_{5-5}}$$

which is the ratio of the power gains of the 90 degree (diagonal) branch and the 0 degree one (straight) coming to the USB output. For the LSB output an analog ratio is defined. Both ratios are presented in Fig. 5. The deviation of the ratios from 1 corresponds to imbalance, which will contribute to the total gain balance error determining the final sideband rejection ratio. The current imbalance is not larger than ±2 dB, which is an acceptable level for achieving the sideband rejection ratio of 10 dB. This measurement can be used as a tool to estimate the IF chain imbalance and quality of sideband separating receivers.

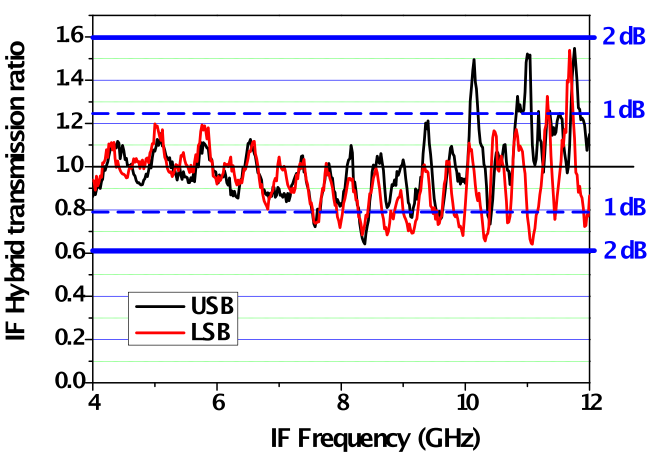

Fig. 5. Ratio of the power transmitted straight and diagonally through the IF hybrid, for both LSB and USB outputs.

The curves in Fig. 5 show a much worse performance than the IF hybrid imbalance determined by manufacturer [4] (2 dB instead of 0.3 dB). This is mainly caused by the transmission ripple of the isolators, and additionally by the interaction of mixers, hybrid and isolators as well as by standing waves between these parts. However, some of these the effects may be exaggerated by the fact that at the used bias points (5 and 8 mV), the output impedances of the SIS devices deviate from their operational design values. In real operation, the mismatches are likely to be smaller.

By biasing both SIS junctions to 5 mV and 8 mV at the same time, the IF noise temperature was determined in the standard way [5][6]. It is in the range from 7 to 12 K in the IF band, as shown in Fig. 6 for one of the IF chains.

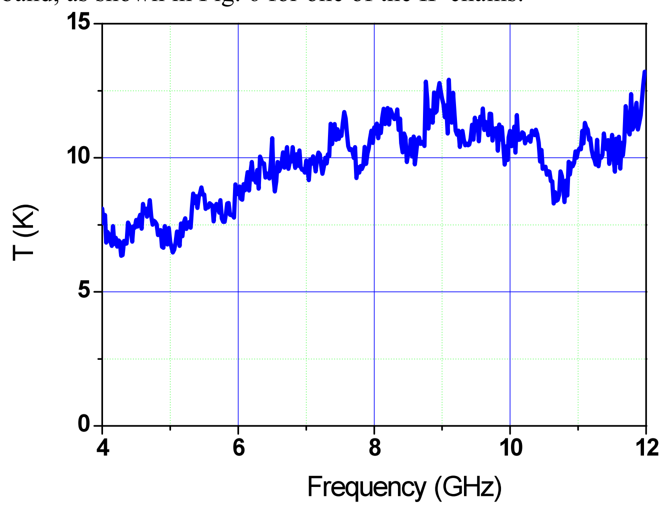

Fig. 6. Noise temperature of the IF chain.

C. Image Rejection Ratio

The image rejection ratio of a sideband separating receiver is mainly determined by the total amplitude and phase error in the hybrids and all components between them. The diagram in Fig. 7 demonstrates how different combinations of these errors contribute to the image rejection level.

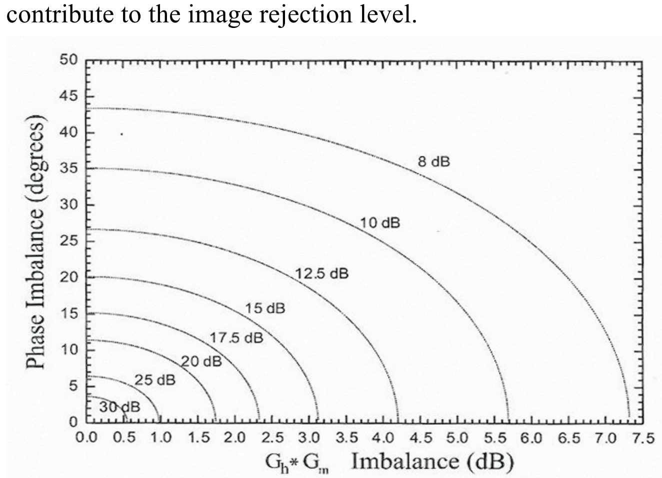

Fig. 7. Theoretical contour lines of equal image rejection as a function of total gain imbalance and total phase imbalance (which include the contributions of RF hybrid, IF hybrid and mixers). Here G_h and G_m are the hybrids and mixers gain imbalances, respectively. [7]

According to the pumping balance measurements presented in Fig. 3 and 5, the upper limit of the combined amplitude imbalance is about 3.5 dB.

The joint phase imbalance of the hybrids is a few degrees and consists of ±2 degrees for the IF hybrid [4] and ±2 degrees for the RF one (based on simulations of the RF hybrid [8]). An additional phase error can appear in case of a length difference between the paths from SIS mixers to IF hybrid input ports. Corresponding cables can be made with a precision of better than 1 mm, which introduces up to 3 degrees phase error for high IF frequencies. All together, phase imbalance should be less than about 7 degrees in total.

Thus, assuming the SIS mixer gains to be equal, the image rejection ratio should be better than 13 dB (according to diagram on Fig. 7). In reality, the gain and phase imbalance of different parts of the receiver may not enhance but compensate each other. Moreover, a compensating amplitude imbalance can be created on purpose by varying the SIS bias voltages, which change the mixer gains.

The ALMA specification for image rejection ratio is 10 dB. We have measured sideband ratio by injecting a test tone RF signal into the upper and lower sidebands. The results for both sidebands are presented in Fig. 8, showing that the image rejection ratio for our mixer is better than 15 dB in the entire range, certainly fitting the ALMA specification. The data presented in Fig. 8 was measured at a fixed bias voltage of 2 mV for both SIS mixers without an additional bias tuning. For the measurements we have used a method described in section III.

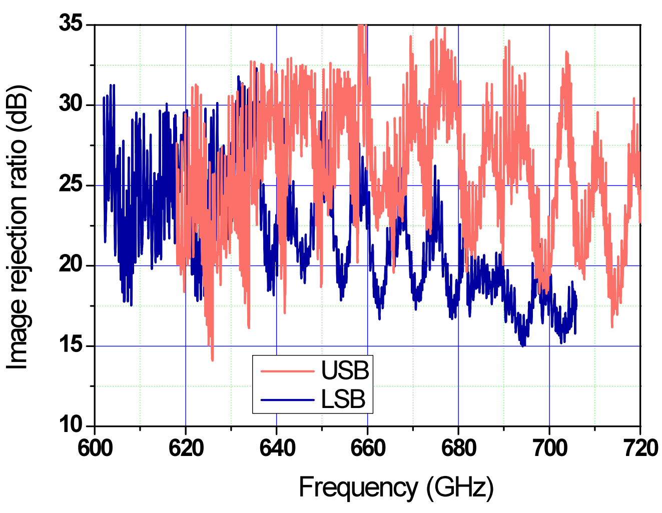

Fig. 8. Image rejection ratio over all RF Band for upper (USB) and lower (LSB) sideband. Each curve consists of 13 IF bands measured for different LO frequencies, spaced 8 GHz apart, yielding a contiguous RF coverage.

D. Noise Temperature

The noise temperature, measured for both lower and upper sidebands using the conventional Y-factor method, is presented in Fig. 9. The best noise temperature is about 330 K. Also plotted in Fig. 9 is the DSB noise temperature of one of the individual junctions, converted to a corresponding ideal SSB noise temperature by scaling it with a factor 2. This way, the shape of the expected curve (in the case of perfect hybrids) can be compared to the actual measurement. Evident from the figure is that the measured data follows the one expected from the DSB data rather closely in shape. However, the overall level of the noise is about 1.8-2 times (2.5 to 3 dB) higher than expected.

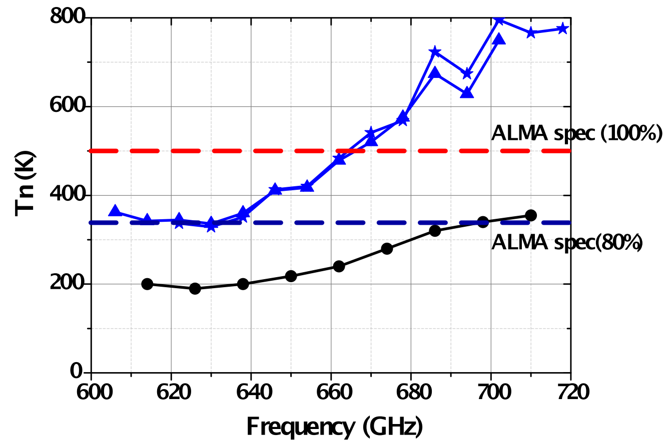

Fig. 9. SSB noise temperature: triangles – lower sideband, stars – upper sideband, circles – the doubled DSB noise temperature of one of the two mixer devices in DSB mode.

The ALMA specifications for single-sideband noise are indicated by the horizontal dashed lines in figure 5: 80% of the band should not exceed 335 K while all points should be below 500 K [9]. In these measurements, the noise temperature is still higher than required.

Additional tests with a standard ALMA Band 9 DSB mixer shows that optics, SIS mixer and IF chain operate properly and do not cause the increase of the observed noise temperature. Therefore, we think that the main reason of the problem is in the RF hybrid block. The frequency independent nature of the noise temperature increase suggests the presence of resistive losses in the waveguide structure. Other defects (mismatches between the blocks, gaps, machining errors) tend to have a strong frequency dependence resulting usually in resonances as demonstrated by electromagnetic simulations. Also, Y-factor measurements through the LO port (instead of the RF port) yield extra losses that scale approximately with the waveguide length. Currently, we are performing an experimental and numerical investigation about the cause of the waveguide losses.

III. Image Rejection Ratio Measurement Method

A. Standard method

A popular method of measuring the image rejection ratio is described in detail in [10]. Here, it will be referred to as a standard method. In this method the test tone (TT) is alternatively injected into the upper or lower RF sidebands and measured at the upper and lower IF outputs.

The sideband separating receiver is depicted schematically in Fig. 10. In this scheme, the upper and lower sidebands of the RF input signal are considered to enter two distinct ports.

The power gains from each RF port to either IF port are denoted by quantities G_{ij}. The image rejection ratios are then: $R_1 = G_{1U}/G_{1L}$ at IF port 1 (USB), and $R_2 = G_{2L}/G_{2U}$ at IF port 2 (LSB).

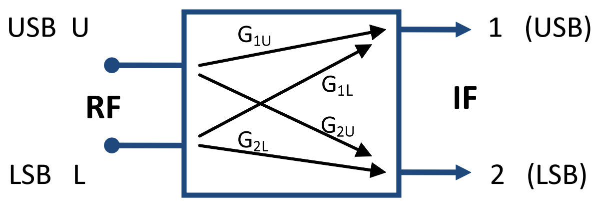

Fig. 10. Power gains of the sideband separating receiver.

R_1 and R_2 cannot be measured directly with a test tone RF signal, because at these frequencies it is difficult to determine with sufficient accuracy the relative amplitudes of two RF signals separated in frequency by twice the IF ($2f_{IF}$ = 8-24 GHz for ALMA receivers). However, the ratios $M_U = G_{1U}/G_{2U}$ and $M_L = G_{2L}/G_{1L}$ can be determined experimentally by injecting a test tone at frequencies $f_{LO} \pm f_{IF}$ and measuring both LSB and USB IF output power. Since the IF output power $P_{IFi,U} = P_{TT}G_{iU}$, with P_{TT} the test tone power, we get

$$M_U = P_{IF1,U}/P_{IF2,U} \,,$$

and similarly for M_L.

When the ratios MU and ML are determined, R_1 and R_2 can be shown to be [10]:

$$R_1 = M_U \frac{M_L M_{DSB} - 1}{M_U - M_{DSB}} \tag{1}$$

$$R_2 = M_L \frac{M_U - M_{DSB}}{M_L M_{DSB} - 1} \,, . \tag{2}$$

M_{DSB} is defined by the ratio

$$M_{DSB} = \frac{\Delta P_1}{\Delta P_2} = \frac{G_{1U} + G_{1L}}{G_{2U} + G_{2L}} \,, \tag{3}$$

where ΔP_1 and ΔP_2 are changes of output power at IF ports 1 and 2, respectively, measured by changing hot and cold loads at the receiver input.

While this method yields accurate results, it has a few disadvantages in our case. In the first place, it requires availability of both sideband outputs, and so it is not usable in an SSB configuration (which we intend for the Band 9 upgrade). Secondly, it requires an accurate calibration of the receiver gains over the IF band for either side band at every LO frequency. This means that at every LO frequency two scans (hot and cold) of over both IF bands have to be performed. This is a rather time-consuming operation, impeding real-time optimization of the image rejection ratio by way of tuning the mixer bias points.

B. Mixer bias inversing method

Because of the SIS junction's antisymmetric I-V curve, biasing one of the SIS mixers to negative voltages gives an additional 180° phase shift in its IF output signal, compared to a positive bias voltage. Such a phase shift causes switching of the USB and LSB after the IF hybrid. This property can be used to construct another method to measure the image rejection, which, under certain conditions, yields values identical or very close to the standard method.

In this method, we measure the following gain ratios:

$$\overline{R}_1 = G_{1^*L}/G_{1L} \text{ and } \overline{R}_2 = G_{2^*U}/G_{2U} \,,$$

Where G_{1L} is the power gain between RF port L and IF port 1 with both mixers biased positively, and G_{1^*L} is the same with the inverted bias of one of the SIS mixers. Correspondingly, G_{2U} and G_{2^*U} are the same ratios for ports U and 2. It should be noted that $\overline{R}_1$ and $\overline{R}_2$ are determined only by inverting the SIS bias voltage, without switching between IF outputs or switching the test tone between two different frequencies (which usually introduces power differences). Results for the bias inverting method ($\overline{R}_1$ and $\overline{R}_2$) in comparison with ratios determined by the standard method (R_1 and R_2) are demonstrated in Fig. 11.

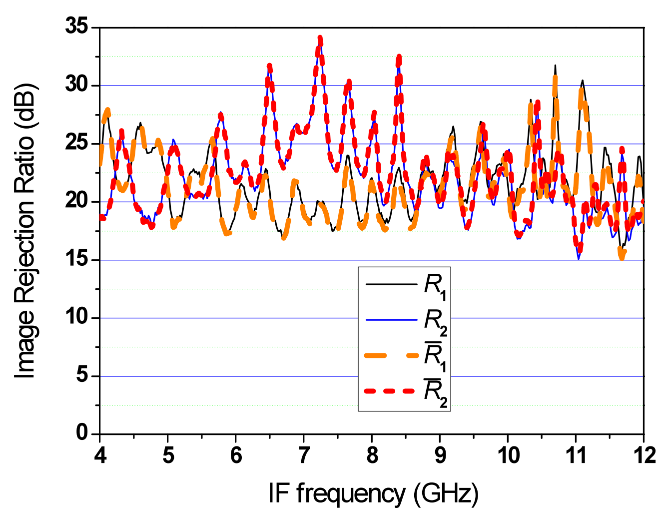

Fig. 11. Image rejection ratio over the entire IF band for a fixed LO frequency (614 GHz). Each curve represents the IF spectrum: solid thin and thick lines corresponds to USB and LSB ratios determined by standard method (R_1 and R_2), long and short dashed lines - LSB and USB ratios find by inverted bias method ($\overline{R}_1$ and $\overline{R}_2$).

The coincidence of $\overline{R}_1$ with R_1 and $\overline{R}_2$ with R_2 on Fig. 11 is a clear confirmation that SIS bias inversion method is precise enough and can be used for characterization of the receiver. The difference between the two methods in this case are less than 1.5 dB. However, it has to be noted that $\overline{R}_1$ and R_1 are not mathematically identical (discussion below will be for $\overline{R}_1$ and R_1, but it is analogous for $\overline{R}_2$ and R_2). The reason is that the denominators (G_{1L}) of the ratios $\overline{R}_1$ and R_1 are the same, but the numerators (G_{1U} and G_{1^*L}) correspond to different signal paths through the IF and RF hybrids, giving a different combination of phase and amplitude errors. Nevertheless, $\overline{R}_1$ and R_1 are similar as shown below.

The ratio R_1 is determined by formula (1), which can be simplified as follows. First of all, we will show that M_{DSB} in our case can be considered as a magnitude of order of 1. The ratio M_{DSB}, determined by formula (3), can be written as

$$M_{DSB} = \left(\frac{g_{1U} + g_{1L}}{g_{2U} + g_{2L}}\right) \cdot \left(\frac{G_{IF1}}{G_{IF2}}\right), \qquad (4)$$

where G_{IFi} are the power gains of the IF chains and $g_{i(U,L)} = G_{i(U,L)}/G_{IFi}$ are the power gains from each RF input port to outputs of the IF hybrid. The first factor of the ratio (4) is determined by the balance of the RF and IF hybrids and similarity of the mixers gains. Its value is of the order of 1 because the hybrids have been determined to be balanced within 2 dB (see Fig. 3 and 5) while the SIS mixers have been selected on their similarity in gain performance. The second factor of the equation (4) is the ratio of the IF gains G_{IFi}, which can be far from 1 in reality. However, it is obvious that SSB-receiver IF gains do not contribute to image rejection ratio. It means that all the G_{IF1} and G_{IF2} appearing in the M_L, M_U and M_{DSB} in (1) or (2) drop out. So, without losing generality, to simplify formula (1) we can consider $G_{IF1}/G_{IF2} = 1$, and then M_{DSB} as a magnitude of order of 1. Taking $M_U, M_L >> 1$ and $M_U >> M_{DSB}$, which is correct for image rejections of the order of 10 ($M_U \sim M_L \sim R_1 \sim R_2$), we can write (1) as

$$R_1 \approx M_L M_{DSB} = \frac{G_{2L}}{G_{1L}} M_{DSB}$$

(M_{DSB} is not completely removed on purpose). The precision of this formula is of order of $1/R_1$ (10% or 0.4 dB for image rejection ratio of 10 dB). Now, to see the difference between $\overline{R}_1$ and R_1 we have to compare G_{1^*L} and the product $G_{2L}M_{DSB}$. For both magnitudes the test tone signal is the same, corresponding to RF port L. The output signals are in proper sidebands (not leaking signals) but in different IF ports 1 and 2, which can be equalized by the calibration factor M_{DSB}, so $G_{2L}M_{DSB} \approx G_{1^*L}$. That bring us finally to $\overline{R}_1 \approx R_1$.

A qualitative explanation for the similarity of $\overline{R}_1$ and R_1 is that the image rejection ratio R_1 is determined mainly by how strong is the leakage from the improper sideband, i.e. by G_{1L}, which is the same for $\overline{R}_1$. The leakage signal amplitude is very sensitive to a small phase or amplitude imbalance in the mixer ($\sim x^2$, $x<<1$) while the relative change of the proper sideband signal is much smaller ($\sim 1+ x^2$). G_{1L} is responsible for the sharp features of the curves R_1 and $\overline{R}_1$ on Fig. 11.

C. *Optimization of the Image Rejection Ratio*

Since the gain of the SIS mixers can be tuned slightly by varying the bias voltage, it is possible to correct for small gain imbalances in the mixers or hybrids, to optimize the image rejection ratio. Fig. 12 shows the IF output powers (both LSB and USB) obtained when injecting a weak TT signal into USB RF sideband. Frequencies of the TT and LO are fixed. One of the mixers is held at constant bias, while the other is swept over a certain voltage range. It can be seen that the power in the proper sideband (curves 1 and 3) hardly varies, while the power of the rejected sideband (curves 2 and 4) shows a clear minimum, demonstrating that the rejection ratio can be optimized. The best bias points in this respect do not necessarily coincide with those yielding the best noise temperature, however.

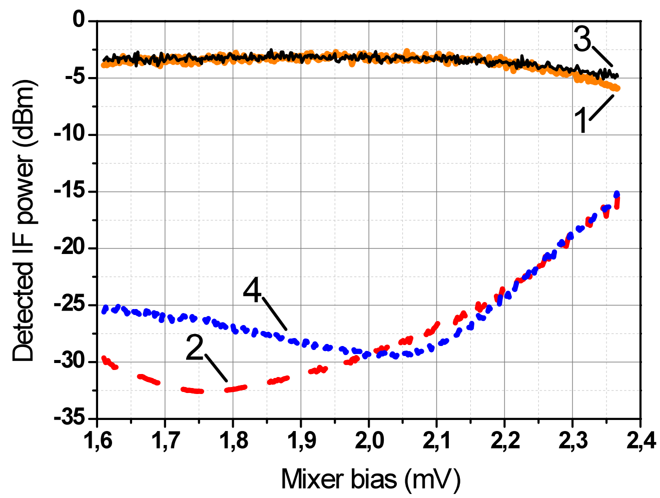

Fig. 12. Dependence of the IF power on the bias voltages of the SIS mixers. The test signal is applied in USB RF sideband. Curves 1 and 2 are the USB and LSB IF powers versus SIS_1 voltage, curves 3 and 4 – USB and LSB IF powers correspondingly versus SIS_2 voltage. Switching of the sidebands is made by inverting the bias voltage of one of the SIS mixers.

IV. Conclusion

We have fabricated and tested a prototype SSB receiver as an upgrade for Band 9. The experimental results are promising. Notably, the image rejection ratio is 15 dB or better in the entire range. The last mixer parameter to be improved to fit ALMA specifications is the noise temperature.

We have also presented in detail the used method for measuring the image rejection ratio. This method is fast, sufficiently precise, gives the possibility of a quick image rejection ratio optimization and works using only one IF sideband.

Acknowledgment

The authors would like to thank Vincent Pierre Desmaris and Victor Belitsky form Chalmers University (Sweden) and Johan Holstein from University of Groningen (Netherlands) for great support and fruitful collaboration. F. P. Mena would also like thank U. Graf from University of Cologne for his advice in machining of the RF hybrid blocks

REFERENCES

[1] R. Hesper, G. Gerlofsma, F. P. Mena, M. Spaans and A. M. Baryshev, “Construction of a Side Band Separating Heterodyne Mixer for Band 9 of ALMA”, Proc. 18th. ISSTT, pp. 39-43, 2007.

[2] J. R. Tucker, .M. J., Feldman, ”Quantum detection at millimeter wavelength”, Rev. Mod. Phys., V. 57., №4., pp. 1055-1113, 1985.

[3] A. V. Khudchenko, R. Hesper, A. M. Baryshev, G. Gerlofma, F. P. Mena, T. Zijlstra, Teun Klapwijk, M. Spaans, J. W. Kooi, “Sideband-separating Mixer for 600–720 GHz”, Proc. SPIE 7854, 78542R, 2010.

[4] I. Malo, J. D. Gallego, C. Diez, I. López-Fernández and C. Briso, “Improved Multi-octave 3 dB IF Hybrid for Radio Astronomy Cryogenic Receivers”, Proc. 20th. ISSTT, pp. 300-306, 2009.

[5] D. P. Woody, R.E. Miller and M.J. Wengler, "85-115 GHz receivers for radio astronomy," IEEE Trans. Microwave Theory Tech., vol. M'IT'-33, pp. 90-95, February, 1985.

[6] N. B. Dubash, G. Pance and M. J. Wengler, “Photon Noise in the SIS detector”, IEEE Trans. Microwave Theory Tech., Vol. 42, №4., pp716-725, 1994.

[7] J.W. Kooi, “Advanced receivers for submillimeter and far infrared astronomy”, PhD thesis, Groningen, 2008, Available: http://dissertations.ub.rug.nl/FILES/faculties/science/2008/j.w.kooi/ThesisJWK-21Nov2008.pdf

[8] F. P. Mena, J. W. Kooi, A. M. Baryshev, C. F. J. Lodewijk, R. Hesper, G. Gerlofsma, T. M. Klapwijk, and W. Wild, “A Sideband-separating Heterodyne Receiver for the 600–720 GHz Band”, IEEE Trans. Microwave Theory and Techniques., V. 59., №1., pp. 166-177, 2011.

[9] W. Wild and J. Payne, “Specifications for the ALMA Front End Assembly”, 2000, Available: http://www.cv.nrao.edu/~awootten/mmaimcal/asac/ALMA_rx_specs_V10.pdf

[10] A. R. Kerr, S. K. Pan and J. E. Effland, “Sideband Calibration of Millimeter-Wave Receivers”, ALMA memo 357, 2001, Available: http://www.alma.nrao.edu/memos/html-memos/alma357/memo357.pdf.